Microphase Separation of Cyclic Block Copolymers of Styrene and Butadiene and of Their Corresponding Linear Triblock Copolymers

Yuqing Zhu and Samuel P. Gido*

Department of Polymer Science & Engineering, University of Massachusetts, Amherst, Massachusetts 01003

Hermis Iatrou and Nikos Hadjichristidis*

Department of Chemistry, University of Athens, Panepistimiopolis Zografou 15771, Athens, Greece

Jimmy W. Mays

Department of Chemistry, University of Tennessee, 655 Buehler Hall, Knoxville, Tennessee 37996-1600

Received August 30, 2002; Revised Manuscript Received October 21, 2002

ABSTRACT: A series of five cyclic block copolymers of styrene and butadiene, having essentially the same molecular weight (52 ± 5 kg/mol) and PS volume fraction varying from 11 to 70%, were synthesized by cyclization of α,ω-dilithium polystyrene−polybutadiene−polystyrene triblock copolymers with bis-(dimethylchlorosilyl)ethane. The cyclic block copolymers thus obtained have practically the same molecular weight and composition as their corresponding linear triblock copolymers. All materials were investigated via transmission electron microscopy (TEM) and small-angle X-ray scattering (SAXS) techniques. In three cases where the cyclic and the corresponding linear block copolymer had the same morphology, the domain spacings of the cyclic block copolymers are found to be 84%−89% of those of their respective linear triblock copolymers. In the other two cases different morphologies are found in the cyclic and its corresponding triblock copolymer. Compared to their linear triblocks, the interfaces are curved away from the connected end blocks.

Introduction

When the two chain ends of a linear ABA triblock copolymer are linked to each other, a cyclic AB block copolymer is formed. The molecular architectures of the ABA triblock and AB cyclic block copolymers are illustrated in Figure 1. Because of their unique closed contour shape, cyclic block copolymers possess distinctively different solution properties[1,2] and microdomain-forming properties[3−7] than linear block copolymer counterparts.

In the microphase-separated states, because of their molecular architecture, an AB cyclic block copolymer can only adopt a double-looped conformation, where both polymer blocks form loops in their respective domains and the two junction points between the blocks reside at the same interface. On the other hand, ABA triblock copolymers can form single loops and/or bridged conformations.[3] Therefore, an ABA triblock copolymer may have its junction points confined at the same interface (loops) or at two different interfaces (bridges). It has been found that[8−10] the percentage of triblock copolymers forming bridges in the lamellar morphology is around 40% over a wide range of χN, where χ is the Flory−Huggins interaction parameter and N the total degree of polymerization.

Cyclic block copolymers have been found to have smaller lamellar long periods than their corresponding linear copolymers. Marko discussed the microphase separation of cyclics and diblock copolymers of the same composition and molecular weight and concluded that the lamellar spacing ratio of a cyclic to its corresponding diblock copolymer is about 0.67 in the strong segregation limit.[11] More recently, Jo and Jang,[5] by using Monte Carlo simulations, found that the ratio of the domain spacing between the cyclic diblock copolymer and the corresponding linear diblock is 0.7. The lamellar spacing ratio was predicted by Thomas et al.[3] to be weakly dependent on χN and to vary between 0.60 and 0.62 for diblock copolymer and between 0.90 and 0.98 for the triblock counterparts. Their experimental results on cyclic PS−PDMS and PS−P2VP and the corresponding triblocks agree well with the prediction. Since the cyclic block copolymers possess a double-looped conformation, a nonnegligible fraction of chain segments must have their trajectories parallel to the lamellar layers in both microdomains. Thus, this fraction of the segments does not contribute to lamellar long period in the normal direction of lamellar, and consequently a decrease in lamellar long period is expected.

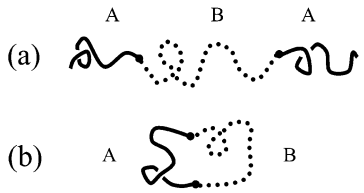

Figure 1. Illustration of an ABA triblock copolymer (a) and an AB cyclic block copolymer (b).

Previous research comparing the domain spacings of the cyclic and triblock copolymers has been limited to lamellar morphologies. The focus of this study is to probe the influence of molecular architecture on their microphase separation behavior across a range of morphologies. A group of α,ω-dilithium polystyrene−polybutadiene−polystyrene (PS−PBD−PS) triblock copoly-

* To whom correspondence should be addressed: e-mail spgido@squeaky.pse.umass.edu or hadjichristidis@chem.uoa.gr.

10.1021/ma021408e CCC: $25.00
Published on Web 12/02/2002

Table 1. Molecular Characteristics of the Cyclic and Triblock Copolymer Precursors

sample[a]	$M_n \times 10^{3}$ [b] (PBD)	$M_n \times 10^{3}$ [b] (copolymer)	M_w/M_n [c] (copolymer)	% PS (w/w)[e] (copolymer)	% PS (w/w)[f] (copolymer)
$(PS-PBD)_C$-11	42.0	47.2	1.06	12	14
PS−PBD−PS-11	42.0	47.5	1.06	14	15
$(PS-PBD)_C$-24	41.5	56.5	1.07	28	32
PS−PBD−PS-24	41.5	55.9	1.07	29	30
$(PS-PBD)_C$-40[g]	32.0	53.5	1.09	*d*	44
PS−PBD−PS-40[g]	32.0	55.1	1.08	*d*	43
$(PS-PBD)_C$-51[g]	23.0	53.4	1.11	*d*	55
PS−PBD−PS-51[g]	23.0	53.0	1.10	*d*	54
$(PS-PBD)_C$-70[g]	16.1	58.0	1.16	*d*	73
PS−PBD−PS-70[g]	16.1	56.9	1.15	*d*	70

[a] Polystyrene block is perdeuterated. [b] Membrane osmometry in toluene at 37 °C. [c] Size exclusion chromatography in THF at 25 °C with a DRI detector. [d] N/A, deuterated polystyrene. [e] Obtained from ^{1}H NMR results in $CDCl_3$ at 25 °C. [f] Size exclusion chromatography in THF at 25 °C with a UV detector. [g] Deuterated PS blocks.

Table 2. Morphological Results of the Cyclic and Their Corresponding Triblock Copolymers

sample	M_n ($\times 10^{-3}$)[a]	f_{PS}[b]	D (nm)[c]	D_C/D_T [d]	morphology
$(PS-PBD)_C$-11	47.5	10.8	32.7		random PS spheres
PS−PBD-PS-11	47.6	10.6	36.8	0.89 ± 0.02	random PS spheres
$(PS-PBD)_C$-24	55.9	24.0	34.6		PS cylinders
PS−PBD−PS-24	56.0	23.9	41.0	0.84 ± 0.02	PS cylinders
$(PS-PBD)_C$-40	55.1	37.8	38.4		lamellae
PS−PBD−PS-40	53.5	39.5	40.3		PS cylinders
$(PS-PBD)_C$-51	51.7	51.2	29.9		lamellae
PS−PBD−PS-51	51.4	51.4	34.6	0.86 ± 0.02	lamellae
$(PS-PBD)_C$-70	56.9	69.6	32.7		PI cylinders
PS−PBD−PS-70	58.0	70.2	55.2		gyroid

[a] Size exclusive chromatography in THF at 30 °C. [b] Determined from ^{1}H NMR results. [c] Determined based the primary reflection of the respective SAXS data. The error for the measurement is ±0.3 nm. [d] Microdomain spacing ratio of that of cyclic to that of its corresponding triblock copolymer.

mers were synthesized anionically. The cyclization reaction was achieved by linking the two living chain ends of the difunctional triblock copolymer precursor under high dilution conditions with an appropriate chlorosilane. By this approach, the contour length and the volume fractions of the cyclic block copolymers obtained are essentially identical with those of its corresponding linear triblock copolymers. Therefore, any morphological difference due to compositional mismatch between the cyclic and corresponding triblock copolymers is eliminated.

Experimental Section

Synthesis. The synthesis of the cyclic and their corresponding triblock copolymers has been presented in detail elsewhere.[12] The molecular characteristics are given in Table 1. The materials are the same as those in ref 12, but a different nomenclature is used here. The subscript "c" used in this study refers to cyclic block copolymer. For example, $(PS-PBD)_C$-11 represents the cyclic block copolymer with 0.11 PS volume fraction, while the PS−PBD−PS-11 refers to its corresponding linear triblock. As indicated in Table 1, cyclics and their corresponding triblock copolymers with 0.40, 0.51, and 0.70 PS volume fractions have deuterated PS blocks while the other materials have protonated PS blocks.

Morphological Characterization. Transmission electron microscopy (TEM) and small-angle X-ray scattering (SAXS) were used to characterize the morphologies of these block copolymers. Specimens for TEM and SAXS were cast from 5 wt % toluene solutions over a period of 14 days. The dried films were annealed under vacuum at 120 °C for an additional 7 days to further promote well-ordered structures. Thin sections 40−80 nm for TEM observation were obtained by cryomicrotoming the annealed bulk films using a Leica EM-FCS microtome, equipped with a crygenic sample chamber operated at −120 °C. These sections were collected and stained with OsO_4 vapor for 4 h. TEM studies were performed using a JEOL 100 CX transmission electron microscope operated at 100 kV. SAXS was performed using Ni-filtered Cu Kα radiation (1.54 Å wavelength) from a Rigaku rotating anode (operated at 40 kV, 200 mA). The X-ray was collimated by a set of three pinholes. A CCD detector (Siemens Hi-Star), located at a camera length of 875.2 mm, was used to record scattering patterns. The morphological characteristics of these cyclic and triblock copolymers based on TEM and SAXS are listed in Table 2.

Results and Discussion

As shown in Table 2, at PS volume fractions of 0.11, 0.24, and 0.51, the cyclics and their triblock copolymer counterparts form the same morphology. On the other hand, comparison of the morphologies of the cyclics and their corresponding triblock copolymers at 0.40 and 0.70 PS volume fractions reveals different microstructures.

PS−PBD−PS-11 and $(PS-PBD)_C$-11 both form the same morphology. The TEM image of $(PS-PBD)_C$-11 in Figure 2a shows PS spheres in an osmium-stained PBD matrix. These microphase-separated PS spheres appear to lack long-range lattice order. Figure 2b shows the small-angle X-ray scattering data of PS−PBD−PS-11 and $(PS-PBD)_C$-11. Both profiles exhibit the primary reflection and one higher-order scattering vector maximum. The primary scattering peak q^* suggests average correlation lengths of 32.7 nm for $(PS-PBD)_C$-11 and 36.8 nm for PS−PBD−PS-11. The higher q reflections in both materials are consistent with form factor scattering maxima from the spherical domains.[13] For comparison, the form factor from spherical domains of the same PS volume fraction as PS−PBD−PS-11 is plotted as a solid line in Figure 2b.

Both PS−PBD−PS-24 and $(PS-PBD)_C$-24 form hexagonally packed PS cylinders in a PBD matrix. The TEM image of cyclic $(PS-PBD)_C$-24 is shown in Figure 3a, where a projection down the axes of the PS cylindrical domains is visible. SAXS data for these two samples in Figure 3b exhibit two Bragg reflections: a primary

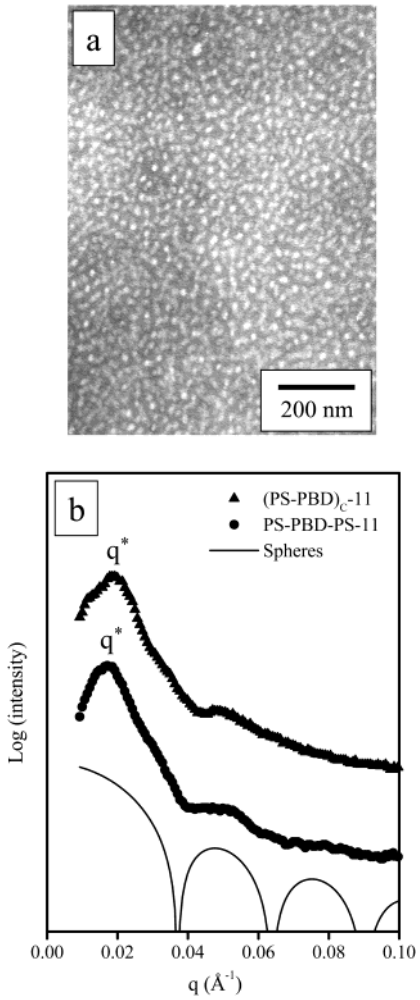

Figure 2. (a) TEM image for (PS−PBD)$_C$-11 cyclic block copolymer. (b) Small-angle X-ray scattering data for cyclic (PS−PBD)$_C$-11 (▲), PS−PBD−PS-11 triblock copolymers (●), and the form factor for spherical domains (—).

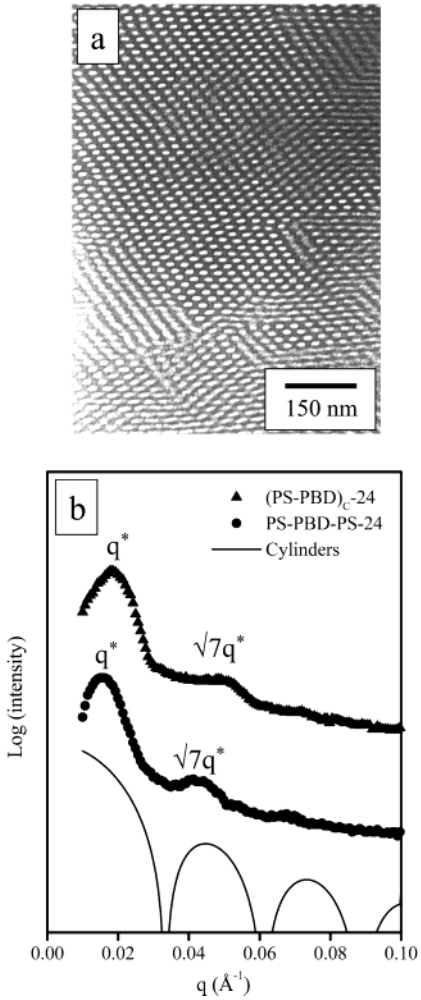

Figure 3. (a) TEM micrograph for (PS−PBD)$_C$-24 cyclic block copolymer. (b) Small-angle X-ray scattering data for cyclic (PS−PBD)$_C$-24 (▲) and PS−PBD−PS-24 triblock copolymers (●) and the form factor for cylindrical domains (—).

peak at q^* and a higher order reflection at $\sqrt{7}q^*$. As also shown in Figure 3b, a cylindrical form factor minimum at the volume fraction of these samples was found to attenuate the expected reflections at $\sqrt{3}$ and $\sqrt{4}$. From this SAXS data, the (100) interplanar spacing is calculated to be 34.6 nm for (PS−PBD)$_C$-24 and 41.0 nm for PS−PBD−PS-24.

Lamellae are observed in TEM images of (PS−PBD)$_C$-51 and PS−PBD−PS-51. Figure 4a shows a TEM image of (PS−PBD)$_C$-51. Small-angle X-ray scattering data for (PS−PBD)$_C$-51 and PS−PBD−PS-51 in Figure 4b display the primary reflection q^* and one higher order reflection at $3q^*$. The absence of the second-order reflections indicates that the volume fractions of both blocks are nearly identical, which is in good agreement with the near symmetric volume fractions. The lamellar long period of (PS−PBD)$_C$-51 and PS−PBD−PS-51 determined by the scattering primary peak q^* is 38.4 and 40.3 nm, respectively.

At PS volume fractions of 0.40 and 0.70, the cyclics and their corresponding triblocks were found to form different morphologies. At 0.40 PS volume fraction, the cyclic (PS−PBD)$_C$-40 forms lamellae, while the triblock PS−PBD−PS-40 forms PS cylinders in a PBD matrix. Figure 5a shows a TEM image of (PS−PBD)$_C$-40, and Figure 5b shows a TEM image of PS−PBD−PS-40. Figure 5c shows the SAXS data for the two samples at 0.40 PS volume fraction. For (PS−PBD)$_C$-40 the observation of integrally spaced Bragg reflections at q^*, $2q^*$, and $3q^*$ is consistent with the lamellar morphology observed via TEM. For PS−PBD−PS-40 reflections at q^*, $\sqrt{7}q^*$, and $3q^*$ are consistent with the TEM observation of hexagonally packed cylinders.

A TEM image of (PS−PBD)$_C$-70 in Figure 6a shows a hexagonally packed PI cylindrical morphology. The SAXS data for (PS−PBD)$_C$-70, shown in Figure 6c, display a higher order peak at $\sqrt{7}$ of the primary reflection q^* consistent with the cylindrical morphology observed with TEM. Figure 6b shows a TEM image of PS−PBD−PS-70. The image indicates a gyroid structure with poor long-range order. Small-angle scattering data of PS−PBD−PS-70 in Figure 6c were only able to give the primary reflection peak. Although this gyroid structure is poorly ordered, a number of characteristic TEM projections were observed. In Figure 6b poorly ordered versions of the "serpentine" and "wagon wheel" projections are visible.[14]

In the three cyclic−triblock material pairs in which the cyclic and its triblock copolymer form the same morphology, microdomain periods of cyclic block copolymers were found to be all smaller than those of the corresponding linear triblock copolymers. This result was found consistently across the three different morphologies observed: PS spheres, PS cylinders, and

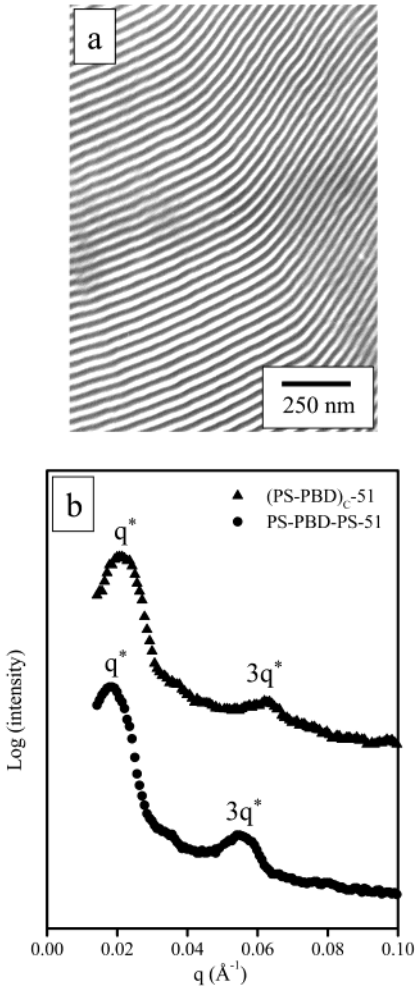

Figure 4. (a) TEM micrograph for $(PS-PBD)_C$-51 cyclic block copolymer. (b) Small-angle X-ray scattering profiles for cyclic $(PS-PBD)_C$-51 (▲) and PS−PBD−PS-51 triblock copolymers (●).

lamellae at PS volume fractions of 0.11, 0.24, and 0.51, respectively. These findings not only support the previous results on lamellar morphologies[3] but also extend this phenomenon to the cylindrical and spherical structures. The domain spacing ratios of cyclic to corresponding triblock copolymer (D_C/D_T) found in this study are given in Table 2. The ratios observed here, between 0.84 and 0.89, are lower than observed or theoretically predicted in the previous study of Thomas et al.[3] where all values exceeded 0.90. The error for SAXS determination of the microdomain spacings is ±0.3 nm, resulting in an uncertainty in the D_C/D_T ratios of ±0.02. The discrepancies between the current results and those of Thomas et al. are beyond the range of this uncertainty.

The series of cyclic and corresponding triblock copolymers used in this study have χN values in the range of 52−81 at room temperature and 40−61 at sample annealing temperature of 120 °C. Actually, the structure observed at room temperature probably reflects the state of the material at the last temperature where there is considerable sample mobility during cooling from the annealing temperature, i.e., the T_g of the PS blocks. However, the χN at the annealing temperature was reported for the PS−PDMS and PS−P2VP cyclic and triblock copolymers in ref 3, and thus we use equivalent conditions for the comparison of our results. The ratios of D_C/D_T obtained in this study are still lower than the theoretical prediction.

When different morphologies are formed by the cyclic and corresponding triblock copolymers, there is a consistent change in the interfacial curvatures with respect to the PS end blocks. The interface curves away from the PS end blocks when they become connected to form a cyclic analogue. In PS−PBD−PS-40, the end blocks stay on the concave side of the interface in the PS cylindrical structure, while the interface in the lamellae of $(PS-PBD)_C$-40 becomes flat. This means that the tendency of the interface to curve away from the PS side is increased by linking the two PS end blocks together. The same effect was also been found in triblock PS−PBD−PS-70, which forms a gyroid structure with PS in the matrix, and cyclic $(PS-PBD)_C$-70, which forms PBD cylinders in a PS matrix. The interfacial curvature of gyroid is intermediate between those of cylinders and

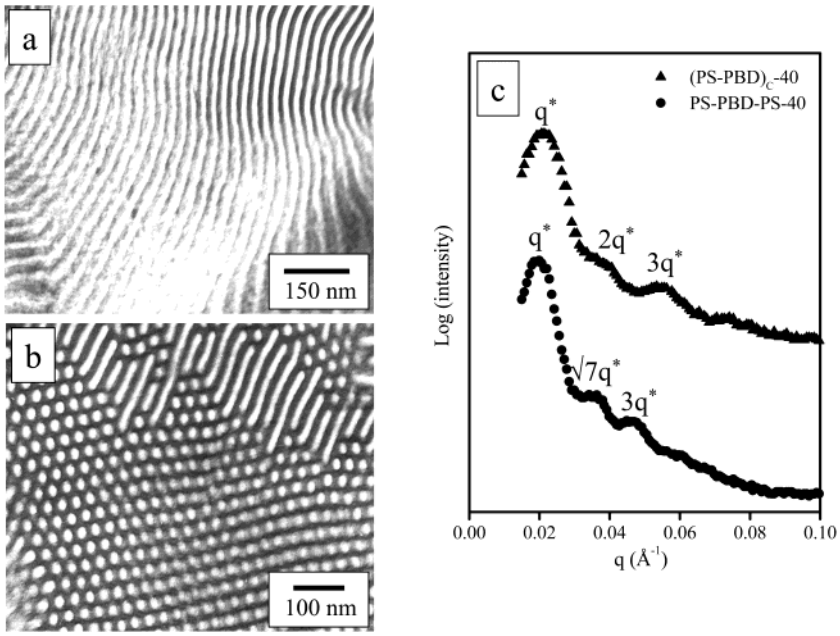

Figure 5. TEM images for $(PS-PBD)_C$-40 (a) and PS−PBD−PS-40 (b) and SAXS data for $(PS-PBD)_C$-40 (▲) and PS−PBD−PS-40 (●) (c).

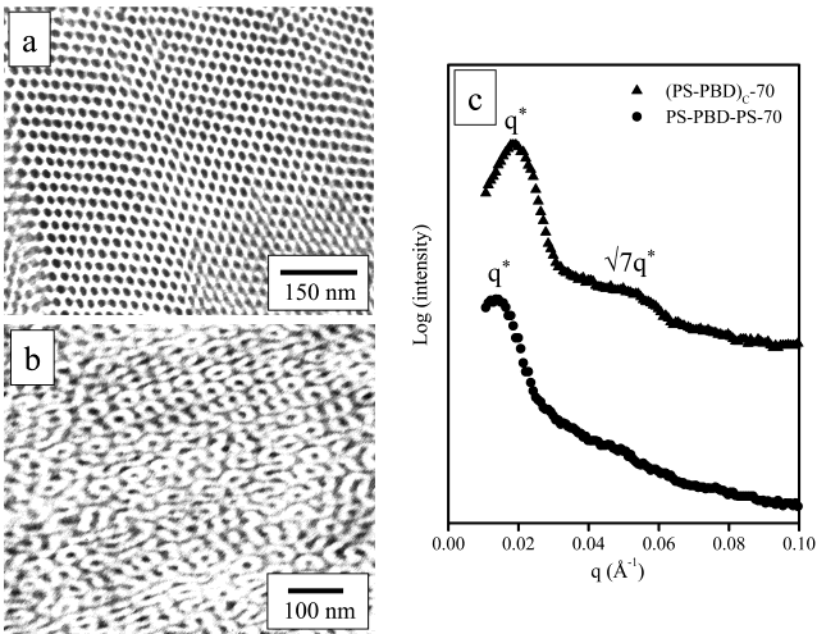

Figure 6. TEM images for $(PS-PBD)_C$-70 (a) and PS−PBD−PS-70 (b) and SAXS data for $(PS-PBD)_C$-70 (▲) and PS−PBD−PS-70 (●) (c).

lamellae. Viewed from the PS (convex) side of the interface, the lower curvature interface of the gyroid in the triblock copolymer changes into the more curved cylindrical interface in the cyclic block copolymer. It is postulated that the same chain trajectory effect that underlies the decrease in domain spacing when going from triblock to cyclic morphologies within the same morphology (PS volume fractions 0.11, 0.24, and 0.51) is also responsible for the change in interfacial curvature that drives morphology changes in samples with PS volume fractions of 0.40 and 0.70. The cyclic requires a PS block chain trajectory component parallel to the interface. This requires more PS chain volume to be located closer to the interface and thus results in a slightly increased tendency for the interface to curve away from the PS side.

Conclusions

The morphological behavior of a series of cyclic block copolymers and their corresponding PS−PBD−PS triblock copolymers has been investigated. The architectural difference of a cyclic and its corresponding triblock copolymers leads to differences in domain spacing. The cyclic morphology always has smaller domain spacing compared to its corresponding triblock copolymer. When cyclic and triblock analogues form different morphologies, it was found that connecting the end blocks of the triblock to form the cyclic tends to increase the tendency for the interface to curve away from the connected end blocks.

Acknowledgment. S.P.G. acknowledges funding from the U.S. Army Research Office under Contract DAAD-19-01-1-0544. We also acknowledge the use of central facilities and the W.M. Keck Electron Microscopy Laboratory in the Material Research Science and Engineering Center (MRSEC) at the University of Massachusetts. H.I. and N.H. acknowledge the Greek General Secretariat of Research and Technology and the Research Committee of the University of Athens for financial support. Financial support from the Graduate Educational Program on "Polymer Science and Its Applications" financed from the Greek Ministry of Education is also gratefully acknowledged.

References and Notes

(1) Amis, E. J.; Hodgson, D. F.; Wu, W. *J. Polym. Sci.: Part B: Polym. Phys.* **1993**, *31*, 2049.
(2) Yu, G.; Yang, Z.; Attwood, D.; Price, C.; Booth, C. *Macromolecules* **1996**, *29*, 8479.
(3) Lescanec, R. L.; Hajduk, D. A.; Kim, G. Y.; Gan, Y.; Yin, R.; Gruner, S. M.; Hogen-Esch, T. E.; Thomas, E. L. *Macromolecules* **1995**, *28*, 3485.
(4) Ryan, A. J.; Mai, S.; Fairclough, J. P. A.; Hamley, I. W.; Booth, C. *Phys. Chem. Chem. Phys.* **2001**, *3*, 2961.
(5) Jo, W. H.; Jang, S. S. *J. Chem. Phys.* **1999**, *111*, 1712.
(6) Mai, S.; Mingvanish, W.; Turner, S. C.; Chaibundit, C.; Fairclough, J. P. A.; Heatley, F.; Matsen, M. W.; Ryan, A. J.; Booth, C. *Macromolecules* **2000**, *33*, 5124.
(7) Morozov, A. N.; Fraaije, J. G. E. M. *Macromolecules* **2001**, *34*, 1526.
(8) Li, B.; Ruckenstein, E. *Macromol. Theory Simul.* **1998**, *7*, 333.
(9) Matsen, M. W.; Schick, M. *Macromolecules* **1994**, *27*, 187.
(10) Watanabe, H. *Macromolecules* **1995**, *28*, 5006.
(11) Marko, J. F. *Macromolecules* **1993**, *26*, 1442.
(12) Iatrou, H.; Hadjichristidis, N.; Meier, G.; Frielinghaus, H.; Monkenbusch, M. *Macromolecules* **2002**, *35*, 5426.
(13) Oster, G.; Riley, D. P. *Acta Crystallogr.* **1952**, *5*, 1.
(14) Alward, D. B. Ph.D. Thesis, University of Massachusetts, 1985.

MA021408E